Journal of Applied Polymer Science

Influences of feeding strategies on AA and MAA carboxylated latexes

Martin Ocepek,[1] Peter Berce,[1] Tina Razboršek,[1] Jožefa Zabret,[1] Lei Meng,[2] Mark D. Soucek[2]
[1]Helios TBLUS d.o.o., Količevo 65, SI-1230 Domžale, Slovenia
[2]Department of Polymer Engineering, The University of Akron, Akron Ohio 44325
Correspondence to: M.D. Soucek (E-mail: msoucek@uakron.edu)

ABSTRACT: Semibatch, power feed, and shot-addition feeding strategies were employed to synthesize carboxylated latex under acidic conditions, using emulsion polymerization. As a source of carboxyl groups, acrylic (AA) or methacrylic acid (MAA) was used. The distribution of carboxyl groups between feeding strategies were investigated using rheology, potentiometric/conductometric titrations, transmission electron microscopy, and FT-IR spectroscopy. Upon alkalization, particle swelling was observed using dynamic light scattering. With increasing pH, both the AA- and MAA-based latexes showed significant increase in hydrodynamic diameter as a consequence of the dissociation state of carboxyl groups. However, only MAA-based latexes exhibit very pronounced increase in viscosity and storage modulus, and were therefore characterized as gels. The effect of feeding strategies was found to be more pronounced with the MAA functionalized latexes. By employing mentioned three procedures, significant differences in the rheological behavior of the neutralized dispersions were detected. © 2015 Wiley Periodicals, Inc. J. Appl. Polym. Sci. **2015**, *132*, 42062.

KEYWORDS: emulsion polymerization; rheology; swelling; synthesis and processing

Received 13 December 2014; accepted 30 January 2015
DOI: 10.1002/app.42062

INTRODUCTION

Feeding strategy represents a strong tool to formulators in designing latexes with desired properties. Emulsion polymerization can be performed batch, semibatch (semicontinuous) or continuous. On industrial scale, semibatch process is most widely used due to its ability to overcome monomer reactivity differences and to ensure sufficient removal of polymerization heat.[1,2] Uniform semibatch (SB) feeding was also upgraded in order to gain control over particle morphology. *Shot-addition* (SA) and *power feed* (PF) strategies were developed to obtain *core-shell* and *gradient* morphologies, respectively.[1–3] Above-mentioned SB, SA, and PF feeding strategies were selected to be compared in this study.

Carboxylic functional monomers are most often incorporated in latex to provide additional electrostatic repulsion, which reduces surfactant amount for latex stabilization.[1] Carboxylic monomers also enhance film properties and compatibility with pigments.[4] Additionally, in thermosetting applications, carboxylic groups can serve as crosslinking sites.[4–8] Acrylic acid (AA) and methacrylic acid (MAA) are far the most commonly used monomers, although itaconic (IA) and fumaric (FA) can also be used in some cases.[9] Of these, MAA was found to be the most successfully incorporated into latex particles, due to its balanced hydrophilic character. Majority of others were found unreacted, placed on the particle surface, or in latex serum as water soluble oligomers.[9,10] The pH of the polymerization media is one of the most important parameters when incorporation of carboxylic acid monomers into/onto latex particles is preferred. That is governed by dissociation state of carboxyl group. Nondissociated form is much more hydrophobic and therefore polymerization is not retarded by electrostatic repulsion.[1,10,11] According to pK_a of carboxylic acid monomers a pH below 4 is required to operate with nondissociate carboxyl groups.[1,10,11] Additionally, polymerization kinetics is also strongly influenced by pH. The propagation rate constant (k_p) decreases from 3150 to 918 $dm^3\ mol^{-1}\ s^{-1}$ at pH 2 and 7, respectively.[11] In latter case, carboxylic groups were found to dominantly stay in latex serum.[10–12] On the other hand initiator (persulfate) decomposition route is also pH dependent. It has been reported that pH <3 will yield in formation of ions instead of radicals.[13]

Successful incorporation of carboxyl groups (COOH) through functional monomers on/in latex particles was found to cause partial particle solvation when neutralization agent was added. As a consequence particle swelling occurred.[10,14–19] The influence on viscosity (known as alkali thickening), with respect to COOH amount and varying comonomer composition, was initially studied by Verbrugge.[14] Viscosity increase was shown to occur when relatively high amounts of MAA (15–30 wt % in monomer composition) were used. High tendency in formation of water-soluble species after neutralization was found in most cases. In those, a peak viscosity was observed on viscosity versus

pH curve.[14] More recently, Zhang *et al.*[15] reported slight decrease in average particle size after alkali thickening, detected by Coulter particle size method. The effect was more pronounced using AA in comparison with MAA. However, only up to 4.5-fold viscosity increase was observed, probably due to AA and MAA represented only 4 wt % in monomer composition.[15] Alkali thickening effect was also observed in a study[16] employing semibatch monomer starved emulsion polymerization. Use of 20 wt % of AA and 6 wt % of Acrylamide in monomer composition yielded some viscosity increase, detected by oscillation rheometry.[16] However, the influences of process strategy on particle morphology, and consequential rheology profiles, were not examined.

The principle of viscosity increase after alkalization (thickening effect) is primary governed by the increase in hydrodynamic diameter of particles. Dynamic Light Scattering (DLS) was found to be a powerful tool to investigate the swelling of carboxylated particles.[18,20,21] On a macroscopic level, swelling strongly affects viscoelastic properties,[19] which can be examined using rheometry analyses.[22] Some alkalized carboxyl latexes exhibit gel-like properties, even though it is assumed that no significant amount of chemical cross-linking knots exists. Physical bonding interactions (e.g., hydrogen bonding, ion-dipole, and dipole-dipole interactions) are responsible for such behavior.[23]

The purpose of this research is to demonstrate influences of feeding strategies on the micro- and macroscopic properties of carboxylated latexes. Semibatch (SB), semibatch monomer *shot addition* (SA), and linear *power feed* (PF) feedings were employed under monomer-starved emulsion polymerization. Acrylic (AA) and methacrylic acid (MAA) were used as the sources of carboxyl groups. Obtained latex dispersions were evaluated using dynamic light scattering (DLS), steady shear and dynamic rheometry, potentiometric and conductometric titrations, transmission electron microscopy (TEM), and Fourier transform-infrared spectroscopy (FT-IR).

EXPERIMENTAL

Materials

Acrylic monomers used were methyl methacrylate (MMA, Sigma–Aldrich), butyl acrylate (BA, Sigma–Aldrich), acrylic acid (AA, Sigma–Aldrich), and methacrylic acid (MAA, Sigma–Aldrich). Before use, inhibitors were removed using Inhibitor removal resin (Alfa Aesar). Producer recommended procedure was followed to remove inhibitors. Sodium dodecyl sulfate (SDS) and ammonium persulfate (APS), both purchased from Sigma-Aldrich, were used as received as surfactant and radical initiator, respectively. pH was controlled using sodium hydroxide (NaOH) and citric acid (CA). For DLS diluents, buffer solutions (purchased from Fluka) were diluted with 0.3 g/L solution of SDS in demineralized (DI) water, until desired conductivity was reached. DI water with conductivity bellow 20 μS/cm was used in all cases.

Synthesis and Characterization Instruments

Syntheses were performed on Optimax™ (Mettler Toledo) working station. Particle size and particle size distributions were measured by dynamic light scattering (DLS) using Zetasizer nano ZS (Malvern). Steady shear and dynamic rheological tests were carried out with Physica MCR 301 (Anton Paar), equipped with fixture PP25 (25 mm diameter plate-and-plate configuration). Titration curves were recorded using the built-in titration features of DT1200 (Dispersion Technology Inc.) coupled with a Jenway 4510 conductivity meter. TEM imaging was performed on JSM-1230 (JEOL). FT-IR spectra were obtained using FT-IR Nicolet 6700 spectrophotometer (Thermo Scientific). Conductivities and pHs were measured using SevenMulti meter (Mettler Toledo). Glass transition temperatures (T_g) were obtained by differential scanning calorimetry (DSC) analysis, performed on a DSC 1 module (Mettler Toledo). Relative densities were obtained with use of hydrometer with 1.000 to 1.100 scale range and graduation of 0.002, respectively. Minimum film formation temperatures (MFFT) were taken using MFFT Bar.60 (Rhopoint Surface Instruments).

Table I. Seed Latex Formulation

	m (g)
DI water	1520.0
SDS	22.5
$NaHCO_3$	7.5
MMA	525.5
BA	224.4
APS	7.5

Seed Latex Synthesis. Seed latex was synthesized using semibatch neat monomer feeding. Ingredient amounts can be found in Table I. DI water, SDS, and $NaHCO_3$ were put into reactor and heated up to 80°C under nitrogen flow. Mixture of monomers was added in a period of 180 min under reduced nitrogen flow.

All following seeded semibatch syntheses were performed using the same master-batch of seeds.

Carboxylated Latex Synthesis. Table II shows synthesis formulations. Working station was equipped with 1 L glass vessel, mechanical stirrer (anchor configuration), a thermocouple, a port for nitrogen purge, a condenser, pH probe, and feeding inlet. The reactor was fed with water, CA, and seed latex. Number of seed particles was chosen to be $(3.7 \pm 0.1) \times 10^{16}$ (1.2×10^{14} per mL of initial water in reactor). Mixture in the reactor was then heated up to reaction temperature (80°C ± 0.1°C) and left for at least 30 min. Meantime, pre-emulsion 1 (P1) was prepared by 10 min mixing of water, monomers, surfactant, buffer, and initiator in a beaker. Before feeding start, APS solution (0.43 g of APS and 5 mL of reactor water) was added into reactor. P1 was feed with continuously with use of peristaltic pump in a period of 3 h. When *power feed* process was used, Pre-emulsion 2 (P2) was feed into P1 with syringe pump. P2 pump rate was set to end 5 min before P1, in order to avoid AA or MAA homopolymerization in water phase. At *shot-addition* process, P2 was shot-added after 50% (1.5 h) of P1 was dosed into reactor.

Table II. Synthesis Formulation

		Control	SB-AA	SB-MAA	SA-AA	SA-MAA	PF-AA	PF-MAA
	Reactor (g)	Pre-emulsion 1 (g)						
Seed	8.39	-						
DI water	305.00	195.00			185.00			
SDS	-	1.55			1.45			
CA	0.11	-						
APS	0.43	1.70				1.59		
MMA	-	93.22	87.12	86.04	87.12	86.04	87.12	86.04
BA	-	119.39	111.57	110.19	111.57	110.19	111.57	110.19
MAA	-	-	-	16.43	-			
AA	-	-	13.92	-				
30% NaOH	0.07	0.15	4.00	1.50		0.05		
		Pre-emulsion 2 (g)						
DI water		-				10.00		
SDS						0.10		
APS						0.11		
MAA					-	16.43	-	16.43
AA					13.92	-	13.92	-
30% NaOH					3.00	1.50	3.00	1.50
Theoretical solids (wt %)		30.25						
Fox calculated T_g (°C)		5.1	10.8	13.0	10.8	13.0	10.8	13.0
Predicted particle density (g/cm^3)		1.12			1.14			
Predicted final particle size (nm)		215			214			

P1 has been subjected to mild stirring (using magnetic stirrer) during entire feeding to insure homogeneous composition, which is mandatory at power feed and shot-addition feeding strategies. It was taken care that pH in all stages of polymerization process was kept between 3 and 4.5 to keep most of carboxylic monomer in nondissociated form. That was ensured by pH controlled addition of NaOH solution into P1, until pH 3.5 was reached with CA/NaOH buffer. Reactor agitator speed was set to 120 rpm to provide enough turbulence to homogeneously distribute the feed, and to prevent phase separation. High nitrogen flow has been applied before feeding. Afterwards, flow rate was reduced to prevent monomer evaporation. After dosing end, reaction mixture was heated up to 90°C and maintained for at least 2 h to achieve maximum conversion. Syntheses were concluded by cooling down to room temperature and pouring latex dispersions into plastic containers.

Characterization

Total overall monomer conversions were determined gravimetrically from solid content; 1 to 1.5 g of hydroquinone quenched samples were weighted into aluminum dish and put in oven at 110°C for 3 h. Samples were then taken out and weighted again. As a result, three replicates were averaged.

Calculations from weight (w) to volume (Φ) solid content was made using eq. (1):[20]

$$\Phi_p = \frac{\frac{w_p}{\rho_p}}{\frac{w_p}{\rho_p} + \frac{w_s}{\rho_s}} \quad (1)$$

where ρ stands for density, and subscripts p and s refer to polymer and solvent, respectively.

Particle Size. DLS measurements were carried out at 25°C and at 173° scattering angle. Samples were diluted bellow 0.1 vol % in order to avoid multiple scattering effects. As diluents, pH 3 to 12 buffer solutions with 0.3 g/L SDS and conductivity of 2.0 mS/cm, were used. Intensity based average particle sizes (D_z) and particle size distributions (PDI) were obtained using Malvern Zetasizer software.

Samples for TEM imaging were diluted with deionized water to approximately 0.1 wt % solids. Latexes were cleaned using a dialysis membrane (MWCO 12,000–14,000) to remove dissolved salts. Cylindrical membrane with diluted sample was closed and placed in a beaker with DI water. Water was replaced every 12 h until the conductivity of the external water was approximately the same as pure deionized water (20 μS/cm).

Rheology. All experiments were performed at 25°C, controlled through a thermostatic system with accuracy of 0.1°C. All reported data were reproducible within 10%. Samples for rheology tests were prepared as follows: dispersions were put as such into a beaker, followed by drop addition of NaOH solution until pH 10 was reached. Homogenization was ensured with use

of magnetic stirrer, and pH was monitored on-line. All rheological measurements were performed 24 h after alkalization.

For the steady shear (flow test), shear rate was step-raised from 0.01 to 1000 s^{-1} in a period of 10 min. Maximum shear rate was then maintained for 4 s, followed by shear rate decrease to starting value with the same time interval as initial increase. Viscoelastic properties were studied by means of storage modulus—G', loss modulus—G'' and their relative comparison—damping factor (tan δ). Strain oscillatory sweep test (ranged from 0.01 to 100% strain at angular frequency 10 rad/s) was first obtained in order to determine linear viscoelastic range (LVO). Frequency oscillatory sweep tests were then performed in a range from 0.1 to 100 rad/s in a period of 5 min.

Potentiometric and Conductometric Titration. Samples for simultaneous potentiometric and conductometric titration were diluted with DI water to 3.0 wt % solids. Neutralization was carried out using 0.5*M* NaOH aqueous solution which was added to approximately 80 mL of diluted latex. All titrations were carried out at 25°C.

FT-IR. Samples were applied manually on the Zinc-Selenide pellet. Spectra at wavelengths between 650 and 4000 cm^{-1}, with resolution of 4 cm^{-1}, were taken.

Conductivity, pH, Glass Transition Temperature, and Relative Density. Conductivity probe was calibrated using certified solution 1413 μS/cm at 25°C and temperature gradient of 1.9%/K. All conductivity results are given at 25°C. pH probe was calibrated with use of certified buffer solutions with pH values of 4.01, 7.00, and 10.00 at 25°C, respectively. T_g was measured on DSC using a heating ramp of 10°C/min in temperature range −70 to 120°C. Relative density was measured by putting latexes and hydrometer into 100 mL graduated cylinder.

RESULTS

The objective of this study was to investigate the location of carboxyl groups in the latex according to feeding procedure of AA and MAA functional monomers. Primary, the influences on DLS hydrodynamic diameter (D_z) and rheological properties, were examined. Additionally, potentiometric/conductometric titrations, TEM imaging, and FT-IR were complementary used to validate proposed intraparticle COOH distribution. In existing open literature[11,14–16] the main focus is being put on the influences of carboxyl amount and comonomer composition. However, the essence of this investigation is to show impact of feeding strategies while maintaining the same monomer composition. Carboxyl composition drift is expected to occur due to changing carboxyl amount at reactor inlet.[1–4,24,25]

Most frequently used conventional semibatch process (under monomer-starved conditions) gives most uniform particle morphology.[1,2,24] However, there are exceptions such as use of hydrophilic monomers which tends to be positioned on/near surface and therefore some intra-particle composition drift can be observed. Shot-addition strategy is basically the most convenient way to design *core-shell* morphology for these types of monomers. The main idea behind this approach is to instantly add functional monomer(s) into feeding mixture at some point

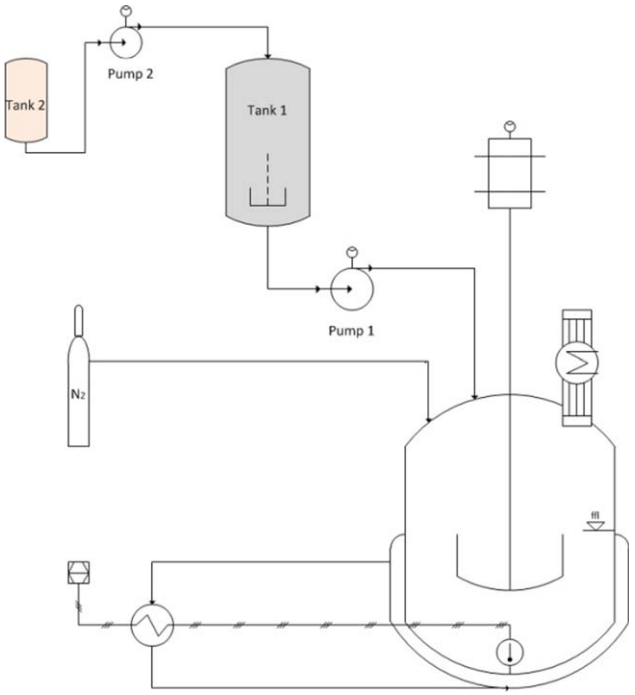

Figure 1. Scheme of linear Power feed semibatch process. [Color figure can be viewed in the online issue, which is available at wileyonlinelibrary.com.]

during classic semibatch feeding. In ideal case, the change in monomer composition will result in corresponding polymer composition. However, thermodynamic tendency might lead to deviations from *core-shell* morphology (e.g. inverted *core-shell*, occlusions, *moon-like*, or even in new generation of particles).[24] *Power feed* semibatch emulsion polymerization process (Figure 1), patented by Bassett and Hoy,[3,25] is an advanced semibatch process. Engineers rely to this polymerization strategy when gradient morphology is of interest.[1,2,11,26] Mathematically, at reactor feeding inlet the concentration of monomer(s) from Tank 2 (Pre-emulsion 2) is increasing following exponential function. Recently, Santillán *et al.*[26] used *power feed* process to synthesize highly carboxylated latexes using AA as functional monomer. Since AA was put in Tank 1, concentration of COOH groups at reactor feeding inlet was decreasing during polymerization course. Due to AA hydrophilicity, higher amounts of carboxyl groups were still found to be on/near particle surface.[26]

In Table III final properties of synthesized latexes are presented. Final solid content coincides with predictions and is comparable among all syntheses. Immediately after the end of feeding, conversion was determined. There were no deviations between feeding strategies. However, MAA latexes were found to have lower conversion at this point in comparison with Control and AA latexes. Relatively low pH in all cases is a result of mandatory low pH process strategy which ensures successful polymerization of AA and MAA.[12,14–16] On the other hand pH above 3 is required to avoid nonradical decomposition of initiator[13] and to keep ionic emulsifier in effective, dissociated form to avoid agglomeration. DLS final particle sizes were very close to designed values presented (see Table II). Polydispersity index (PDI) show very narrow distribution according to practical criteria.[27,28] Conductivities are comparable among samples, minor

Table III. Final Properties of Latex Dispersions

	Control	SB-AA	SB-MAA	SA-AA	SA-MAA	PF-AA	PF-MAA
Solids (wt %)	30.2 ± 0.1	30.2 ± 0.1	30.1 ± 0.1	30.2 ± 0.1	30.1 ± 0.1	30.2 ± 0.1	30.2 ± 0.1
Final monomer conversion (%)	99.8 ± 0.3	99.8 ± 0.3	99.7 ± 0.3	99.8 ± 0.3	99.6 ± 0.3	99.8 ± 0.3	99.8 ± 0.3
Monomer conversion at dosing end (%)	97.9 ± 0.3	97.2 ± 0.3	94.2 ± 0.3	97.0 ± 0.3	93.4 ± 0.3	97.1 ± 0.3	93.4 ± 0.3
pH (/)	4.00 ± 0.02	4.34 ± 0.02	3.82 ± 0.02	4.13 ± 0.02	3.72 ± 0.02	3.91 ± 0.02	3.75 ± 0.02
Final D_z (nm) at pH 4	210 ± 5	212 ± 2	209 ± 4	217 ± 4	214 ± 2	215 ± 3	212 ± 1
DLS PDI at pH 4	0.017	0.017	0.010	0.041	0.025	0.028	0.005
Conductivity\ (mS/cm)	7.15 ± 0.05	4.67 ± 0.05	3.64 ± 0.05	4.45 ± 0.05	3.97 ± 0.05	4.01 ± 0.05	3.67 ± 0.05
T_g DSC (°C)	2 ± 1.0	10 ± 0.3	16 ± 0.4	9 ± 0.3	8 ± 0.8	8 ± 0.5	16 ± 2.0
MFFT (°C)	<0	<0	9 ± 1	<0	7 ± 2	<0	9 ± 1
Relative density (/)	1.034 ± 0.002	1.038 ± 0.002	1.038 ± 0.002	1.038 ± 0.002	1.038 ± 0.002	1.038 ± 0.002	1.038 ± 0.002

deviations can be attributed to slight variations of pH. T_g of AA containing latexes are lower in general due to AA homopolymer T_g of 130°C while MAA homopolymer has T_g of 162°C.[1] As a consequence, MFFTs of MAA latexes are higher, while MFFTs of Control and AA latexes were even below water freezing point.

DLS Hydrodynamic Particle Size

Figure 2 represents D_z dependence with respect to pH of diluents. Control latex (containing no carboxyl groups) shows no significant increase in D_z with respect to increasing pH. Therefore it was used as a reference. AA-based latexes gave similar DLS response with SB as with PF synthesis process, while SA resulted in the largest extent of apparent particle swelling among AA latexes. Even more significant differences among feeding strategies were detected at MAA latexes. At pH 10, use of SA process yielded most pronounced particle swelling. D_z of 333 nm is notably bigger in comparison with 297 nm and 252 nm at PF and SB strategies. As a consequence, particle volumes (and volumetric solid content) increased for 377%, 275%, and 175%, respectively.

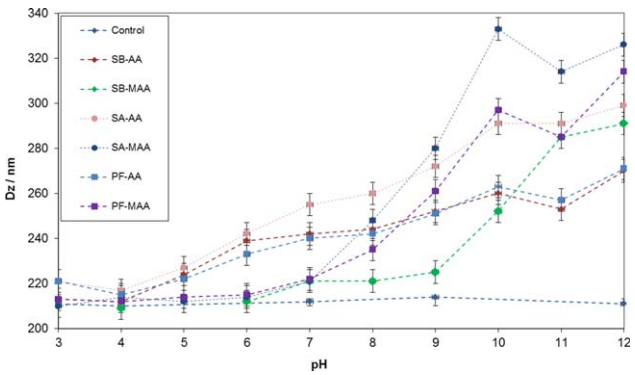

Figure 2. pH dependence of hydrodynamic radius. Dotted line is drawn for easier following. [Color figure can be viewed in the online issue, which is available at wileyonlinelibrary.com.]

Rheology

Figures 3 and 4 represents rheology flow curves of neutralized dispersions. pH 10 was found to give highest swelling in most dispersions. For the sake of comparison, pH 10 was selected for rheology characterization. It is kept in mind SB-MAA could develop additional viscosity increase at higher pH, although it is still be lower in relation to SA-MAA and PF-MAA. Flow curve comparison in Figure 3 reveals that only 10 mol % of carboxylic monomers in composition yields 6 orders of magnitude increase in viscosity. When using MAA all three feeding procedures

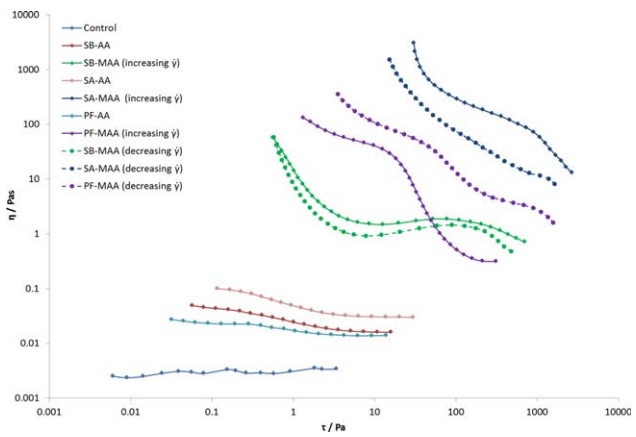

Figure 3. Influence of shear rate on viscosity for neutralized dispersion samples at pH 10. Control and AA-based samples are not time-dependent (identical results for $\dot{\gamma}$ increase or decrease). [Color figure can be viewed in the online issue, which is available at wileyonlinelibrary.com.]

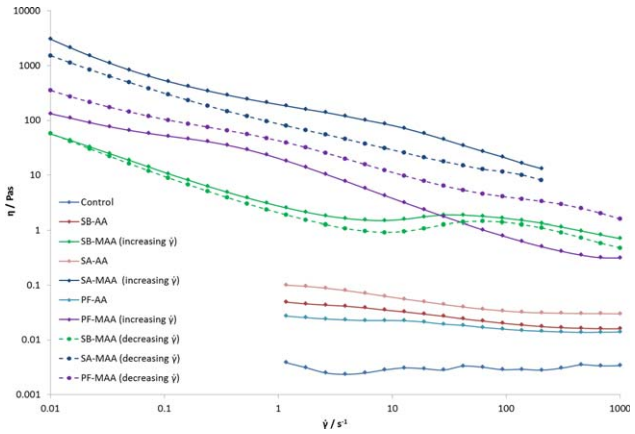

Figure 4. Influence of shear stress on viscosity for neutralized dispersion samples at pH 10. [Color figure can be viewed in the online issue, which is available at wileyonlinelibrary.com.]

yielded gel-like structure after latex alkalization. On the other hand, the use of AA did not result in gel-like structure in any case. However, viscosity was still up to 100 times higher in comparison with control sample which was not pH dependent.

Figures 3 and 4 also show that viscosity of latexes without gel-like structure (control, SB-AA, SA-AA, and PF-AA) does not significantly change with shear stress (or shear rate). Although, slight pseudoplasticity is observed with all AA syntheses, while the control latex exhibit pure Newtonian flow behavior. All the mentioned latexes show the same rheological profile during shear rate increase or decrease, meaning they are not time dependent. On the other hand, gel-like (MAA-based) latexes can be classified as non-Newtonian viscoelastic fluids.[22] SA-MAA and PF-MAA are pseudoplastic in entire measured shear rate, while SB-MAA becomes dilatant above shear rate of 10 s^{-1}. All MAA latexes are also time dependent. SB-MAA and SA-MAA are thixotropic and PF-MAA is rheopectic. One can observe the usage of three feeding strategies and two carboxylic monomers was enough to obtain all the main rheological behaviors with respect to shear rate and time variable.[22]

Following one of basics definitions for gels—domination of G' over G'' at frequency sweep test, and gel appearance itself,[22,23] gel-like structures at pH 10 can are only observed with the MAA latexes. Figure 5 represent oscillatory amplitude sweep tests which were obtained in order to determine linear viscoelastic region (LVR). LVRs of 2, 5, and 8% were determined for SB-MAA, SF-MAA, and PF-MAA, respectively. Frequency sweep test (Figure 6) was performed with strain amplitude set to 1%. As expected,[22] storage (G') and loss modulus (G'') both tends to increase with increasing ω. SA-MAA was found to yield highest structure, while SB-MAA and SA-MAA are comparable. Figure 6(b) represents damping factor G''/G' ratio, expressed as tan δ.

TITRATIONS

Results of conductometric titrations of SB samples are shown in Figure 7. Control latex sample shows initial steady conductivity, followed by a sharp rise above 0.2 mL of NaOH. The slope in the second region is the same as obtained by titration of DI water. AA based latexes had higher overall conductivity in comparison with MAA. Conductometric results for SA-AA and PF-AA were practically identical to SB-AA while SA-MAA and PF-MAA displayed slightly higher overall conductivity than SB-MAA. In all cases, the equivalent point at about 5 mL (0.0028 mol_{NaOH}/L) of NaOH indicates that all the acid groups, incorporated during synthesis, were neutralized during titration. This was also verified by checking pH values of the neutralized samples three days after titrations had been carried out. Changes in pH were in the range of 1% and therefore considered as insignificant.

Potentiometric titrations of SB syntheses are compared in Figure 8 and corresponding derivatives in Figure 9. Degree of ionization (α_n) is defined as quotient between NaOH instant consumption and NaOH consumption at equivalent point, obtained from conductometric titrations:

$$\alpha_n = \frac{n_{\mathrm{NaOH}}}{n_{\mathrm{NaOHeq.}}} \tag{2}$$

The differences between curves of AA and MAA-based latexes are significant; up to $\alpha_n \sim 0.3$, AA latexes [Figures 8(a) and 9(a)] requires higher α_n to reach comparable pH to MAA latexes [Figures 8(b) and 9(b)]. In $0.3 < \alpha_n < 1.0$ region, slope of MAA curves is significantly reduced. At and above $\alpha_n \sim 1.0$, no significant differences between AA and MAA was observed. As best seen from Figure 9, two inflection points were detected at AA, and a single one at MAA latexes.

Even though polyacids (e.g. carboxylated latexes) lack a single dissociation constant, regions between the inflection points can be used to estimate the ionization dependent effective dissociation constant (pK_{eff}).[11,29] Figure 10 shows values calculated using eq. (3):

$$pK_{\mathrm{eff}} = \mathrm{pH} + \log_{10}\left(\frac{1-\alpha_n}{\alpha_n}\right) \tag{3}$$

The calculated pK_{eff} are much higher in comparison with typical carboxyl acids. That is a consequence of electrostatic interaction between the ionized carboxyl groups, and probably also because

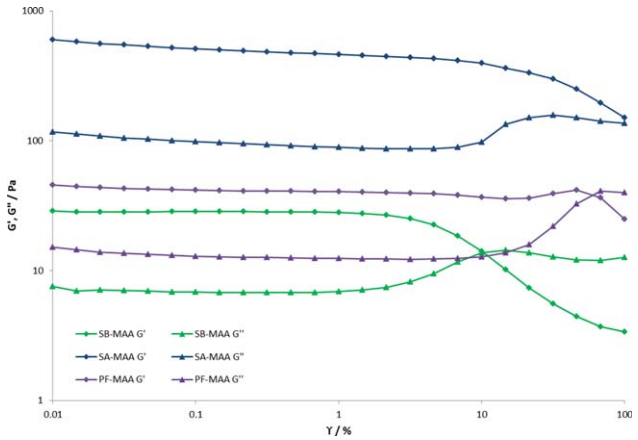

Figure 5. Amplitude sweep test results for gel-like samples at pH 10. [Color figure can be viewed in the online issue, which is available at wileyonlinelibrary.com.]

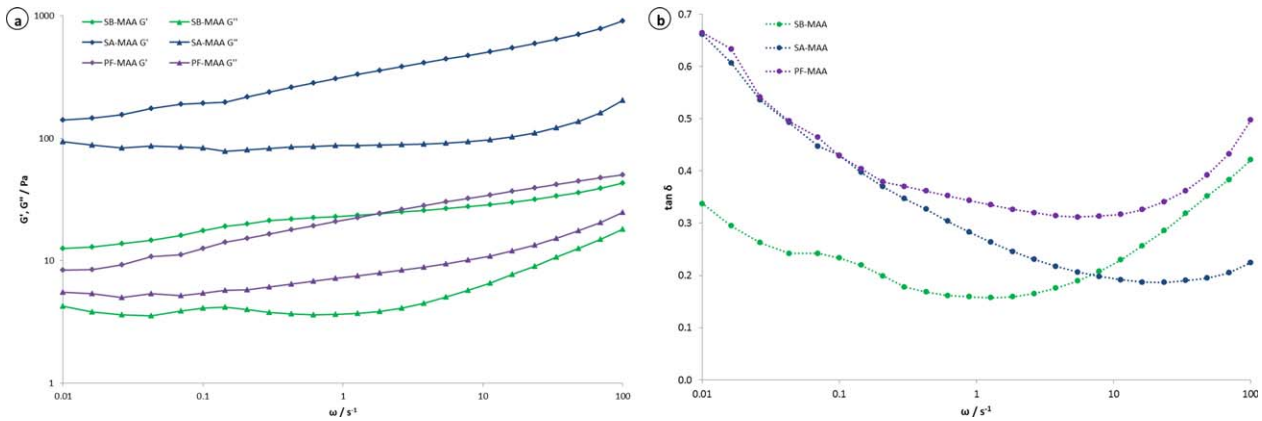

Figure 6. G' and G'' (a) and tan δ (b) frequency dependence of gel-like samples at pH 10. [Color figure can be viewed in the online issue, which is available at wileyonlinelibrary.com.]

of the rigid, nonpolar surroundings beneath the particle surface.[11,29]

Transmission Electron Microscopy

TEM images (Figure 11) were also taken in order to exclude presence of secondary nucleation,[30] and to confirm proposed morphology of latex particles. No secondary particles were observed in any case. When AA was used [Figure 11(b,d,f)] no significant composition drift was observed. On the other hand, gradient contrast suggests gradient morphology of MAA containing latex particles, especially at SA and PF processes [Figure 11(e,g)]. Although, basic TEM imaging is hard to be used as independent method in latex applications,[31] results are consistent with DLS, rheology and titration results.

FT-IR

Figure 12 shows FT-IR spectra comparison. The focus of the spectra was on the carboxylic C═O stretch which can be found at wavenumber range 1700 to 1720 cm^{-1}.[32] No carbonyl stretch at control latex was detected, since it did not contain any carboxylic acid. On the other hand, the presence of carbonyl group was detected in all other latexes. Comparable carbonyl absorbance can be used as internal reference for relative comparison in a region below 1700 cm^{-1}. SB-MAA had the highest absorbance in that region, while SA-MAA had some lower and PF-MAA the lowest, among MAA latexes. The same trend can also be observed at AA based latexes.

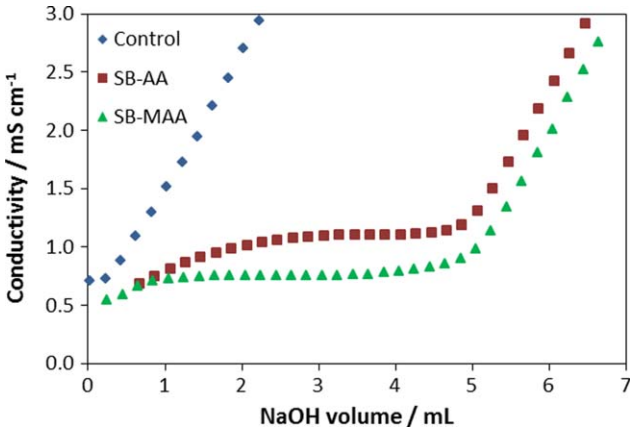

Figure 7. Conductivity versus volume of 0.5*M* NaOH added. Comparison between AA and MAA using SB process. [Color figure can be viewed in the online issue, which is available at wileyonlinelibrary.com.]

DISCUSSION

Majority of industrial latexes contain at least some carboxylic monomers, in most cases to improve stability through electrostatic repulsion. Occasionally higher amounts of carboxylic monomers are used to emphasize latex thickening.[15,16,19] Influences of pH on carboxyl partitioning and polymerization kinetics were extensively studied.[10,11,14,15] However, process procedure can also have enormous influence on particle morphology and consequential final material properties.[3,12,26] In most academic studies, batch or semibatch process is used, without putting much focus on process parameters sensitivity. Therefore, the primary aim of this study was to show influences that monomer feeding strategies (semibatch, *shot-addition* and *power feed*) have on final carboxylated latex dispersions. Feeding strategies were found to have major influence on swelling, titration curve and FT-IR spectra, resulting in considerably different rheological properties.

The focus in experimental design was to formulate functional latex with applicable rheology properties, eliminating the need for external thickeners in coating formulation. Solid content of 30 wt % is high enough to be commercially used. On the other hand it is low enough to eliminate most of the influences on rheology properties, arising from particle crowding.[1,22] APS solution shot, followed by pre-emulsion feeding in a period of 3 h ensured monomer starved conditions; 2h postreaction at elevated temperature ensured practically maximum possible conversion (see Table III). Constant particle number during the polymerization course was reached using monodisperse seed latex and proper surfactant dosing during feeding. No agglomeration or secondary nucleation was observed in any case, confirmed by TEM. Instantaneous conversion at the end of feeding (see Table III) was some lower at MAA-functionalized latexes. Apparent higher polymerization rate of AA latexes can be

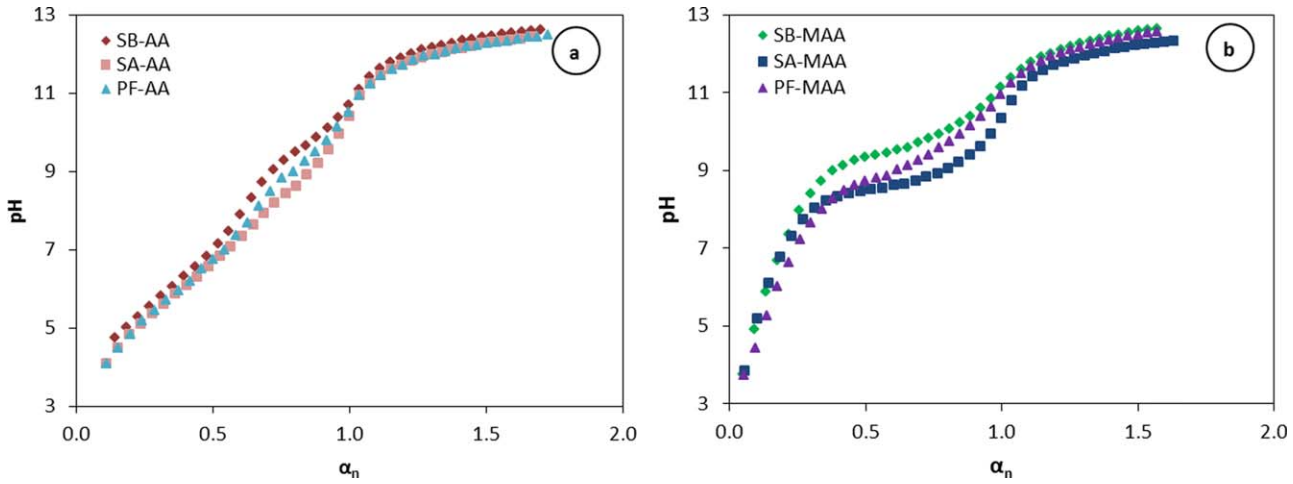

Figure 8. Influences of feeding strategies on potentiometric titration curve: a) AA and b) MAA latexes. [Color figure can be viewed in the online issue, which is available at wileyonlinelibrary.com.]

attributed to higher AA hydrophilicity and consequential partial homo-polymerization in water phase.[9,10,26] Nevertheless, final conversion was not affected.

Increase of average particle size after alkalization, obtained by DLS (Figure 2), is somehow contradictory with one of the previous published investigations,[15] where reduced average particle size was reported. That is obviously governed with the use of Coulter particle size analyzer which is based on polarization intensity differential scattering.[33] In contrast to DLS, where average hydrodynamic radius is obtained,[18,20,21] Coulter particle analyzer apparently detects only nonswollen particle size. Therefore, authors agree that DLS method is more appropriate to study swelling of carboxylated latexes. Table IV represents increase in hydrodynamic particle size between pH 4 and 10. Using eq. (1), latex volume solid content in acidic form can be calculated. In order to show effect of swelling, apparent volume solids at pH 10 can be calculated by simple multiplying:

$$\Phi_p(\text{pH } 10) = \Phi_p(\text{pH } 4) \times \left(D_{\text{pH } 10}/D_{\text{pH } 4}\right)^3 \quad (4)$$

where it should be emphasized that calculated values serves only as relative comparison between latexes.

Swelling phenomena on particle level was evidently detected by DLS. However, influences on macroscopic properties were yet to be investigated. Comparable D_z (and apparent Φ_p) increase for all AA and MAA latexes at pH 10 implies similar rheological behavior. However, flow curves (Figures 3 and 4) neglect that assumption. Even though AA-based latexes show some increase in viscosity, only use of MAA yielded in highly-structured liquids (gels) with several orders of magnitude of viscosity increase. Authors attribute majority of D_z increase of AA based latexes to increase in Debye radius,[1,34] while most of D_z increase of MAA-based latexes arise from inter-particle swelling, as the result of MAA partitioning.[10] Proposed behavior is presented on Figure 13. MAA gels were further investigated with frequency sweep tests (Figure 6). The reason that SA feeding yielded most structured viscoelastic liquid[22] is probably in best

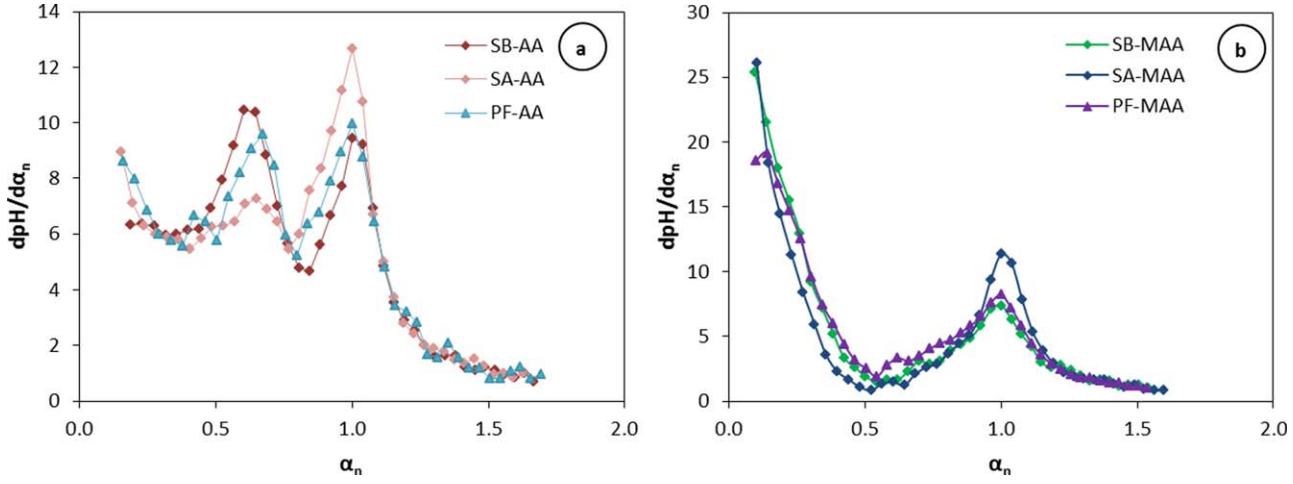

Figure 9. First derivative of a) AA and b) MAA potentiometric titration curves. [Color figure can be viewed in the online issue, which is available at wileyonlinelibrary.com.]

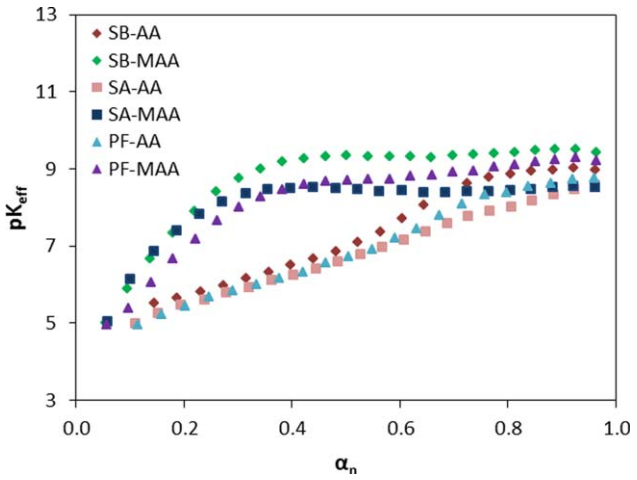

Figure 10. Effective dissociation constant values versus the degree of neutralization. [Color figure can be viewed in the online issue, which is available at wileyonlinelibrary.com.]

carboxyl distribution among used strategies. It can be concluded that SB puts too much carboxyl groups in the inner and PF to the outer layer of particles. One can make that assumption according to calculated carboxyl concentration at reactor feeding inlet. Within MAA functionalized dispersions, significantly different time dependent rheological behavior was observed. While thixotropic behavior with SB-MAA and SA-MAA was expected, the rheopectic behavior of PF-MAA (Figures 3 and 4) indicates irreversibility of shear deformed particles.[22] PF process obviously puts most of the carboxyl groups near surface and applied shear helps to untangle very hydrophilic MAA-rich chains, which tend to stay extended in water phase, acting as a thickener. Tan δ presented in Figure 6(b) show domination of storage over loss modulus in the whole measurable frequency range. Similar trend is observed with PF-MAA and SA-MAA, while at SB-MAA neutralized dispersion G′ is more dominant. However, differences are not significant.

Synthesized dispersions were further characterized via titrations, as it is often the case with carboxylated latexes.[11,14,16] Comparison of conductometric titration curves within SB syntheses (Figure 7) show differences as the consequence of monomer compositions. It was surprising that NaOH consumption at the end of second inflection points was the same as predicted from formulation recipe and holds for all samples. That means all introduced carboxyl groups were neutralized. It proves that interparticle diffusion is not limiting factor in latex neutralization step. Potentiometric titrations presented in Figures 8 and 9 reveal even more significant differences between AA and MAA based latexes. Curves for AA fall into three regions, separated by two inflection points [Figure 8(a)]. According to Quadrat *et al.*,[35] the first inflection point corresponds to neutralization of acid groups located on the surface of the latex particles and water soluble oligomers, while the second inflection point indicates groups buried beneath the surface of the particles. By subtracting the amount of acid, determined for the Control sample, the mole fraction of carboxyl groups on surface and in water phase oligomers was determined to be between 50% and 55% for AA latexes. The lowest fraction of surface COOH groups was found using SB strategy while PF pushes most COOH on the surface. That is consistent with uniform, step-increased and exponential changes of carboxyl concentration at reactor inlet for SB, SA, and PF processes, respectively. Unlike AA, potentiometric curves of MAA based latexes [Figure 8(b)] lack the first segment. A reliable determination of the first inflection point is therefore difficult. However, by examination of potentiometric curves it can be concluded that the surface and water phase oligomer carboxyl groups comprise about 5%

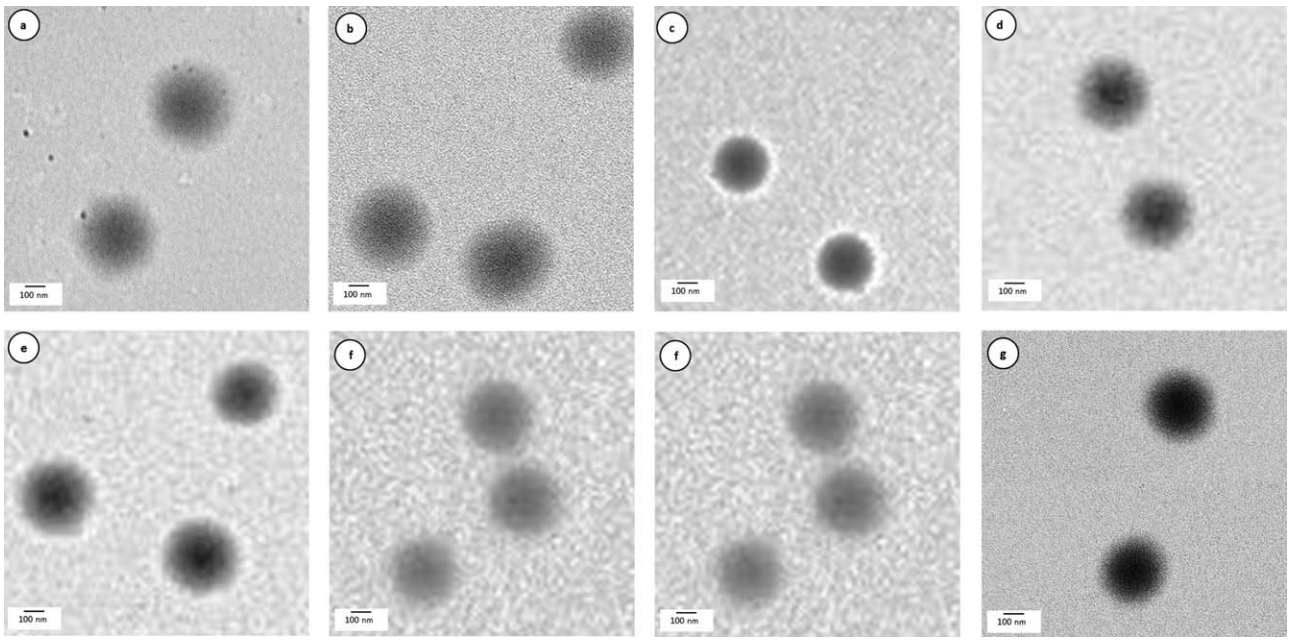

Figure 11. TEM images. a) Control, b) SB-AA, c) SB-MAA, d) SA-AA, e) SA-MAA, f) PF-AA, and g) PF-MAA.

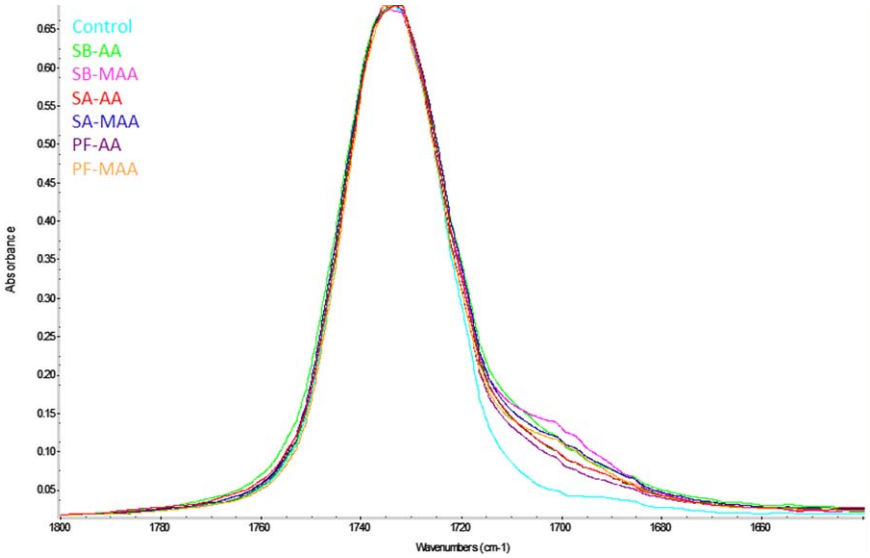

Figure 12. Partial FT-IR spectra. [Color figure can be viewed in the online issue, which is available at wileyonlinelibrary.com.]

of all carboxylic groups in PF-MAA and even less for SB-MAA and SA-MAA latexes. Differences in feeding strategies are less significant, although the trend is identical in comparison with AA. SB feeding tends to yield inflection point at lowest degree of neutralization, followed by PF and SA, respectively. Beside morphology differences, this phenomenon can be attributed to increasing molecular weight.[36]

Figure 10 offers additional aspect on latex comparison. SB-MAA has the highest p$K_{a\text{eff}}$ which corresponds to swelling at pH 9 and up. The same observation can be seen from DLS (see Figure 2). SA-MAA swells the most of all MAA latexes and has the lowest effective pK_a. Again, DLS and rheology profile confirms that thesis. The sloping p$K_{a\text{eff}}$ for PF-MAA could indicate gradient in the shell (in contrast to SB-MAA and SA-MAA which have a relatively constant p$K_{a\text{eff}}$ in the region between inflection points). Higher pK_a means that the acid dissociates with more difficulty. This is attributed to: (a) electrostatic interaction with neighboring ionized groups and (b) nonpolar/rigid surroundings which could possibly obstruct ionization.[11,29] On the exterior part of particles, only (a) is probable and a steep p$K_{a\text{eff}}$ is evident (observed for AA based latexes). The logical assumption leads to conclusion that a higher degree of ionization has a stronger effect on p$K_{a\text{eff}}$, while MMA-BA polymer matrix (b) should not have significant effect when AA was used, and at PF-MAA. On the other hand, ionization of the interior groups of SB-MAA and SA-MAA are mostly governed by the matrix effect (b). That can be contributed to different particle morphologies. The highest fraction of interior groups, determined by the lower inflection point and the p$K_{a\text{eff}}$ of the interior region, occurs with SB, followed by SA and the PF (true for all latexes with AA and MAA). This finding is also consistent with DLS results (Figure 2) which is also revealing that AA in formulation causes particles swelling already at pH around 5, while MAA shifts beginning of swelling to pH 7 at SA-MAA and PF-MAA, or to pH 9 at SB-MAA. Beside particle morphology, monomeric pK_a of AA 4.26, with respect to MAA pK_a of 4.65,[9,11,36] could have some contribution, although that effect can be neglected in high molecular weight polyacids.

Previously discussed differences in morphology were also observed by TEM microscopy. Even though relatively soft particles represent a challenge to get reliable images, differences in particle contrasts indicates gradient to *core-shell* morphology. The latter seems to be most pronounced at SA-MAA [Figure 11(e)] and PF-MAA [Figure 11(g)]. That is consistent with DLS, rheology, and titration data. The highest FT-IR absorbance of SB-MAA in carboxyl group region (Figure 12) is another indicator of carboxyl group distribution—higher absorbance indicates more homogeneous morphology. PF-AA therefore possesses most nonuniform morphology, meaning most of carboxyl groups are concentrated on surface. Absorbance trend $A_{SB} > A_{SA} > A_{PF}$ is valid for both, AA and MAA.

Table IV. Comparison of Volume Solids According to DLS Results

	Control	SB-AA	SB-MAA	SA-AA	SA-MAA	PF-AA	PF-MAA
ΔD_H pH = 4–10 (nm)	4 ± 2	48 ± 7	43 ± 10	74 ± 5	119 ± 14	48 ± 4	85 ± 12
Φ_p pH = 4 (vol %)	27.4 ± 0.1	27.5 ± 0.1	27.4 ± 0.1	27.5 ± 0.1	27.4 ± 0.1	27.5 ± 0.1	27.5 ± 0.1
Φ_ppH = 10 (vol %)[a]	29.0 ± 0.8	50.7 ± 4.1	48.0 ± 5.7	66.3 ± 3.5	103.3 ± 13.6	50.3 ± 2.3	75.6 ± 9.5

[a] Apparent volume solid content.

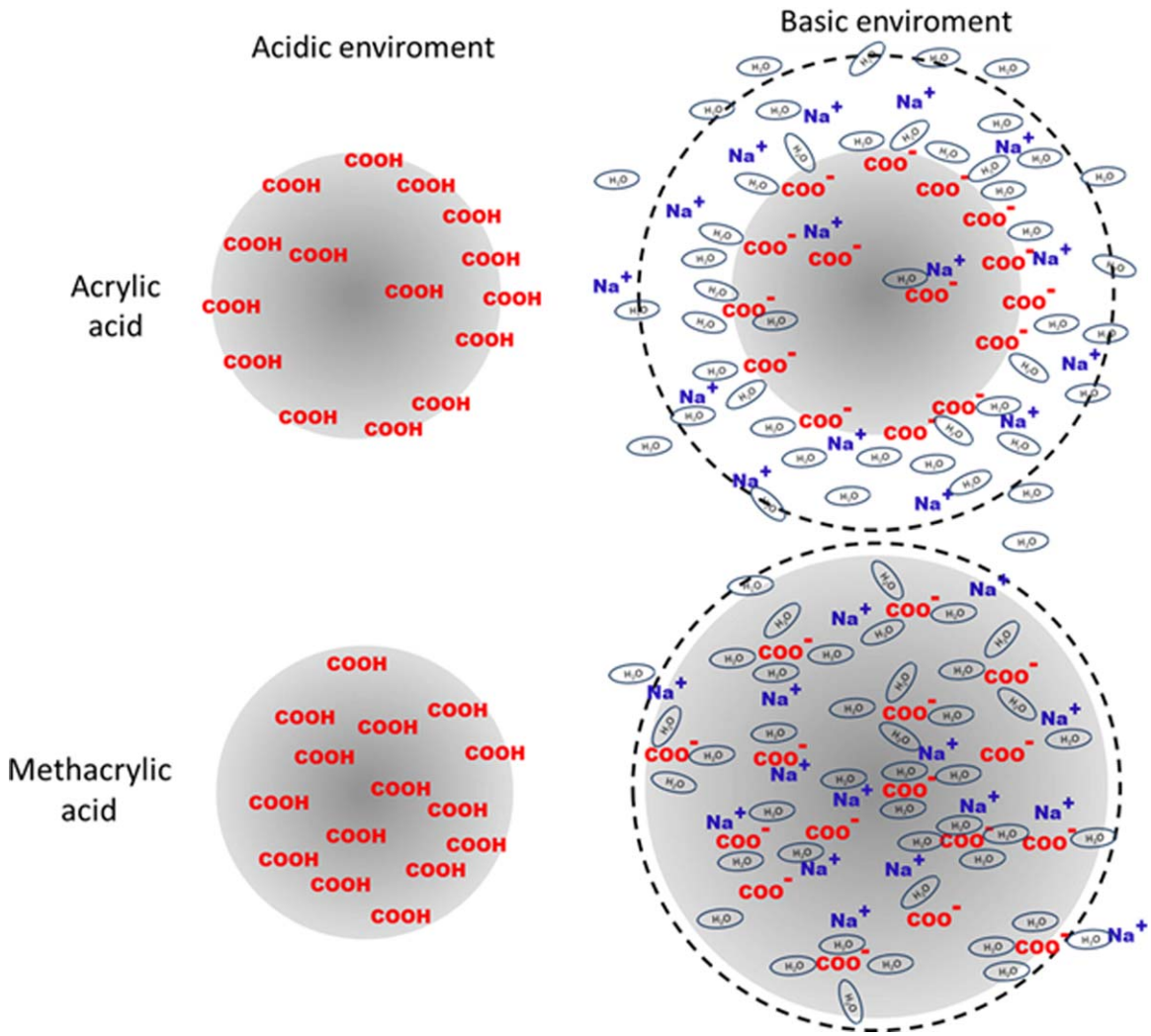

Figure 13. Schematic illustration of AA and MAA particle swelling after alkalization with NaOH. Dotted line represents the same apparent Hydrodynamic particle size, obtained by DLS. [Color figure can be viewed in the online issue, which is available at wileyonlinelibrary.com.]

Carboxyl functionalized latexes requires multi-disciplinary approach. They can be described as polymer, colloid, or even gel. Feeding strategies inside semibatch emulsion polymerization process were found to offer a wide window for formulators to synthesize various carboxylated dispersions with pronounced rheological properties. Additional finding from this study relates to differences between solvation of MAA and AA functionalized latexes (see Figure 13). It was found the main reason for increased Hydrodynamic diameter of AA based latexes is pronounced solvation of shell-located carboxyl groups, while MAA-based dispersion possesses intraparticle solvation, resulting in true particle swelling. Therefore DLS show approximately the same particle size increase after alkalization, while viscosity and mechanical modulus increase is only observed when MAA was used. Proposed morphologies were also validated by titrations, TEM and FT-IR.

CONCLUSIONS

Carboxylated latexes were synthesized using semibatch, *power feed*, and *shot-addition* feeding strategy with 10 mol % of acrylic or methacrylic acid, as functional monomers. DLS analysis revealed increase in hydrodynamic particle size in all obtained latexes. However, steady shear and oscillation rheology tests of alkalized dispersions revealed that only MAA latexes exhibit gel-like structure, while use of AA provide only neglectable amount of storage modulus increase. *Shot-addition* feeding was found to yield most structured liquid, followed by *power feed* and semibatch feeding strategy. According to titration results, MAA distribution tends to be process dependent. On the other hand, feeding strategy had neglectable influence on AA-based latexes, due to thermodynamical driving force which push AA units closer to the particle surface. As consequence, only MAA was found to be efficient in obtaining appropriate carboxyl group distribution in order to obtain structured liquids after neutralization.

This operation was part financed by the European Union, European Social Fund. The operation was implemented in the framework of the Operational Program for Human Resources Development for the Period 2007–2013. Priority axis 1: Promoting entrepreneurship and adaptability.

REFERENCES

1. Lovell, P. A.; El-Aasser, M. S. Emulsion Polymerisation and Emulsion Polymers; Wiley: Chichester, **1997**.
2. Herk, A. Chemistry and Technology of Emulsion Polymerisation; Blackwell Publishing: Oxford, **2005**.
3. Bassett, D. R.; Hoy, K. L. U. S. Pat. 3804,881, **1974**.
4. Wicks, Z. Jr.; Jones, F.; Pappas, S. P. Organic Coatings Science and Technology; Wiley: New York, **2007**; Vol. *3*.
5. Pedraza, E. P.; Soucek, M. D. *Eur. Polym. J.* **2007**, *43*, 1530.
6. Wu, S.; Soucek, M. D. *Polymer* **2000**, *41*, 2017.
7. Teng, S.; Soucek, M. D. *Polymer* **2001**, *42*, 2849.
8. Serkan, B.; Soucek, M. D. *React. Funct. Polym.* **2013**, *73*, 291.
9. Oliveira, M. P.; Giordani, D. S.; Santos, A. M. *Eur. Polym. J.* **2006**, *42*, 1196.
10. Santos, A. M.; Mckenna, T. F.; Guillot, J. *J. Appl. Polym. Sci.* **1997**, *65*, 2343.
11. Kawaguchi, S.; Yekta, A.; Winnik, M. A. *J. Colloid Interface Sci.* **1995**, *176*, 362.
12. Slawinski, M.; Schellekens, M. A.; Meuldijk, J.; Herk, A. M.; German, A. L. *J. Appl. Polym. Sci.* **2000**, *76*, 1186.
13. Johnson, R. L.; Tratnyek, P. G.; Johnson, R. O. *Environ. Sci. Technol.* **2008**, *42*, 9350.
14. Verbrugge, C. J. *J. Appl. Polym. Sci.* **1970**, *14*, 897.
15. Zhang, X.; Fu, H.; Huang, H.; Cheng, H. *J. Wuhan Univ. Technol.* **2010**, *25*, 492.
16. Santos, Z. M.; Neto, A. O. W.; Dantas, T. N. C.; Pereira, M. R.; Fonseca, J. L. C. *Eur. Polym. J.* **2007**, *43*, 3314.
17. Vesaratchanon, J. S.; Takamura, K.; Willenbacher, N. *J. Colloid. Interface Sci.* **2010**, *345*, 214.
18. Bradna, P.; Stern, P.; Quadrat, O.; Snuparek, J. *Macromolecules* **1997**, *30*, 482.
19. Quadrat, O.; Mrkvickova, L.; Walterova, Z.; Stern, P.; Bradna, P.; Snuparek, *J. Prog. Org. Coat.* **2003**, *46*, 1.
20. Saunders, B. R.; Vincent, B. *Adv. Colloid Interface* **1999**, *80*, 1.
21. Saunders, B. R.; Crowther, H. M.; Vincent, B. *Macromolecules* **1997**, *30*, 482.
22. Mezger, T. G. The Rheology Handbook, 3rd ed.; Vincentz Network: Hannover, **2011**.
23. Katsuyoshi, N. *Progr. Colloid. Polym. Sci.* **2009**, *136*, 87.
24. Chern, C. S. *Prog. Polym. Sci.* **2006**, *31*, 443.
25. Bassett, D. R.; Hoy, K. L. Emulsion Polymers and Emulsion Polymerization, ASC Symposim Series No. 165; American Chemical Society: Washington, **1981**.
26. Santillán, R.; Nieves, E.; Alejandre, C. P.; Gómez-Yañez, C.; Río, J. M.; Dorantes-Rosales, H.; Navarro-Clemente, M. E.; Corea, M. *J. Ind. Eng. Chem.* **2013**, *19*, 1257.
27. International Standard ISO13321. Particle Size Analysis – Photon Correlation Spectroscopy; International Organization for Standardization (ISO), Geneva, Switzerland, **1996**.
28. International Standard ISO22412, Particle Size Analysis: Dynamic Light Scattering (DLS), International Organization for Standardization (ISO), 2008.
29. Borkovec, M.; Koper, G. J. M.; Piguet, C. *Curr. Opin. Colloid Interface Sci.* **2006**, *11*, 280.
30. Ocepek, M.; Soucek, M. D.; Berce, P.; Lei, M. *Macromol. Chem. Phys.* **2015**, *216*, 400.
31. Gaillard, C.; Fuchs, G.; Plummer, C. J. G.; Stadelmann, P. A. *Micron* **2007**, *38*, 522.
32. Vanderberg, J. T. An Infrared Spectroscopy Atlas for the Coating Industry; Federation of Societies for Coatings Technology: Chicago, **1980**.
33. Keck, M. C. Cyclosporine Nanosuspensions: Optimised Size Characterisation & Oral Formulations, Ph.D. Thesis; Freie Universität Berlin: Berlin, **2006**.
34. Hiemenz, P.; Rajagopalan, R. Principles of Colloid and Surface Chemistry; CRC Press: New York, 1997.
35. Quadrat, Q.; Mrkvičková, L.; Walterová, Z.; Titkova, L.; Bradna, P.; Šňupárek, J. *Colloid. Polym. Sci.* **1998**, *276*, 879.
36. Dong, H.; Du, H.; Qian, X. *J. Phys. Chem. B* **2009**, *113*, 12857.